Accelerated Publications

A One-Residue Switch Reverses the Orientation of a Heme *b* Cofactor. Investigations of the Ferriheme NO Transporters Nitrophorin 2 and 7 from the Blood-Feeding Insect *Rhodnius prolixus*†

Fei Yang,‡ Hongjun Zhang,‡ and Markus Knipp*,§

Department of Chemistry, The University of Arizona, 1306 East University Boulevard, Tucson, Arizona 85721-0041, and Max-Planck-Institut für Bioanorganische Chemie, Stiftstrasse 34-36, D-45470 Mülheim an der Ruhr, Germany

Received October 30, 2008; Revised Manuscript Received November 28, 2008

ABSTRACT: This study represents the identification of a single amino acid residue that has the major responsibility for the isomeric orientation of a heme *b* cofactor in a ferriheme protein. The insertion of hemin *b* into the asymmetric environment of a protein pocket facilitates two cofactor orientations, **A** and **B**, which is often called "heme rotational disorder". The proteins studied herein are nitrophorins, a class of ferriheme proteins found in the saliva of the blood-sucking insect *Rhodnius prolixus*, in this case NP2 and NP7. NMR spectroscopy (pH* 5.5) of the imidazole complex of NP7 revealed solely the **A** orientation, whereas NP2 shows primarily the **B** orientation (∼1:5 **A**:**B**). The glutamate 27 residue in NP7 is an obvious difference in the heme pocket compared to those of NP1−4, all of which present a valine residue [valine 24 (NP2 and NP3) or valine 25 (NP1 and NP4)] at the same position. Consequently, the mutant NP2(V24E) was prepared and shown to reverse the heme orientation to exclusively **A**, whereas NP7(E27V) revealed an ∼1:3 **A**:**B** ratio. The reversal **A** ↔ **B** following the change glutamine ↔ valine was further indicated in circular dichroism (CD) spectroscopy with a positive (**A**) or negative (**B**) $\Delta\varepsilon$ of the heme Soret band. Moreover, CD spectroscopy was applied to the mutant NP7(E27Q) and indicated mainly the **A** orientation, which allows us to conclude that the steric hindrance provided by the glutamate residue is responsible for the heme orientation rather then the carboxylate charge.

Since heme *b* lacks 2-fold symmetry, two orientations (**A** and **B**) in the pocket of a hemoprotein are possible, both of which are displayed in Scheme 1. NMR spectroscopy frequently reveals that both orientations are present in solution, as indicated by two sets of paramagnetically shifted ^{1}H heme resonances in systems with non-zero electron spin. This phenomenon, well-known as "heme rotational disorder", has been observed in many heme *b*-containing proteins (ref *1* and references cited therein). It was found that the **A**:**B** ratio depends strongly on the individual heme protein. For instance, **B** is the major orientation in sperm whale myoglobin (Mb)[1] (*2*), whereas in bovine cytochrome b_5, a ratio of ∼8:1 (*3*) and in *Chironomus thummi thummi* HbIII a ratio of ∼1.1:1 is observed (*4*). Another class of heme proteins

Scheme 1: Isomeric Orientations **A** and **B** in NP2 from *R. prolixus*[a]

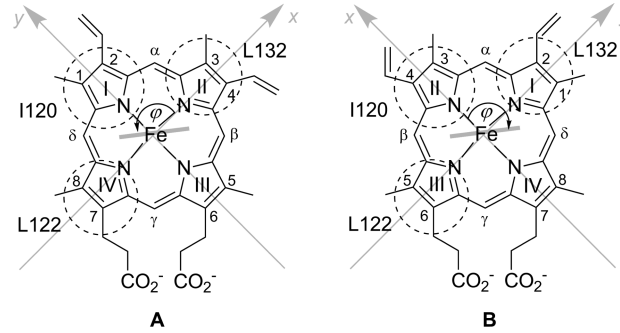

[a] The view is from the distal side with His-57 (gray bar) behind the heme. Substituents on the periphery of the heme are numbered clockwise from the methyl 1 (1M) to the methyl 8 (8M) for the **A** orientation. The pyrrole rings are numbered from I to IV with the *y*-axis defined going through the N_I-Fe-N_{III} motif. Dashed circles denote the positions of three distal aliphatic site chains indicated pointing onto the heme plane.

† This study was supported by the Swiss National Science Foundation (SNF), Grant PA00A--109035, and the Grossmann-Stiftung of the Max-Planck-Institut für Bioanorganische Chemie (to M.K.).

* To whom correspondence should be addressed. Phone: +49 (0)208 306 3581. Fax: +49 (0)208 306 3951. E-mail: mknipp@mpi-muelheim.mpg.de.

‡ The University of Arizona.

§ Max-Planck-Institut für Bioanorganische Chemie.

[1] Abbreviations: CD, circular dichroism; DEA/NO, (*Z*)-1-(*N*,*N*-diethylamino)diazen-1-ium-1,2-diolate; Hb, hemoglobin; Hm, histamine; HMQC, heteronuclear multiple-quantum coherence; ImH, imidazole; L, ligand bound to heme iron; MALDI, matrix-assisted laser desorption ionization; Mb, myoglobin; MOPS, 3-(*N*-morpholino)propanesulfonic acid; NOESY, nuclear Overhauser enhancement spectroscopy; NP, nitrophorin; rmsd, root-mean-square deviation; TOF, time-of-flight; WEFT, water-eliminated Fourier transform; *wt*, wild-type.

10.1021/bi8020229 CCC: $40.75
Published on Web 12/22/2008

in which the heme orientation has been extensively studied by NMR spectroscopy in recent years is the nitrophorins (NPs) (*5*−*10*). The NPs represent a group of ferriheme *b* proteins found in the blood-sucking insect *Rhodnius prolixus*, designated NP1−4 (*11*) and NP7 (*12*). The purpose of these proteins is to store NO in the salivary glands and then to transmit it as a signal to increase blood-vessel diameter and to inhibit blood coagulation of the host during feeding; upon NO release, the imidazole group of histamine (Hm) binds to the open coordination site of the iron, and thus, the sequestration of Hm contributes to the suppression of the immune response (*13*). The structure of NP is unique for heme proteins, in that the heme is located at the open end of a β-barrel (*14*), rather than in the more commonly observed, largely α-helical globin or four-helix bundle folds. The ferriheme prosthetic group is bound to the protein via a His ligand, leaving the sixth iron coordination site available to bind NO or other ligands. Only in the case of NP4 was the presence of both orientations observed by X-ray crystallography (*15*), while NMR spectroscopy revealed either an approximately equal distribution of both isomers (NP1 and NP4) or the preference for the heme **B** orientation (NP2 and NP3) (*5*−*10*).

For NP7, an experimental structure is not yet available. However, a homology model for NP7(G3-S182) (*16*) was built on the basis of the X-ray structure of NP2 (*17*), with which NP7 shares a level of amino acid sequence identity of 61%[2] (rmsd = 0.39 Å) (*16*). Because of the uncertainty of the heme orientation in NP7, iron 3,7,8,12,13,17-hexamethyl-21*H*,23*H*-porphine-2,18-dipropionate (2,4-dimethyldeuterohemin or "symmetrical hemin") was inserted into the model structure. During the inspection of the homology model of NP7 (*16*), Glu-27 attracted our interest. This position in the sequence is represented by a Val residue in NP1−4, which is indicated in the amino acid sequence alignment in Figure 1A (arrow). In each of the 31 crystal structures of *wt* NP1, -2, and -4 currently available in the Protein Data Bank, the orientation of Val-24/25 is similar, as depicted in Figure 1B. Thus, hydrophobic interaction of the isopropyl moiety with the vinyl and methyl substituents of heme pyrrole ring I or II, depending on the orientation of the cofactor (compare Scheme 1), is established. In this respect, the presence of the carboxylate moiety together with the increased side chain length introduced by Glu-27 is remarkable. Figure 1C shows that the side chain of Glu-27 faces the hydrophobic side of the heme (pyrroles I and II) where the Glu-27 $C^{\delta}OO^{-}$ group is positioned in the distal heme pocket. Thus, the question of the influence of this residue on the properties of the heme cofactor arises. To address this question, the mutant NP7(E27V) was generated to model the situation in NP1−4. Further, to examine the role of the Glu carboxylate, the charge-depleted mutant NP7(E27Q) was constructed. Concomitantly, the reverse mutant NP2(V24E) was produced to identify the effect of the Glu residue in the context of another NP structure.

[2] Although NP3 is the protein most similar to NP7 (62% level of amino acid sequence identity), the slightly less similar NP2 (61% level of amino acid sequence identity) was chosen for comparison because it is much better characterized (e.g., NP3 is the only isoprotein of NP1−4 for which no X-ray structure has been reported). This is also true with regard to NMR spectroscopy.

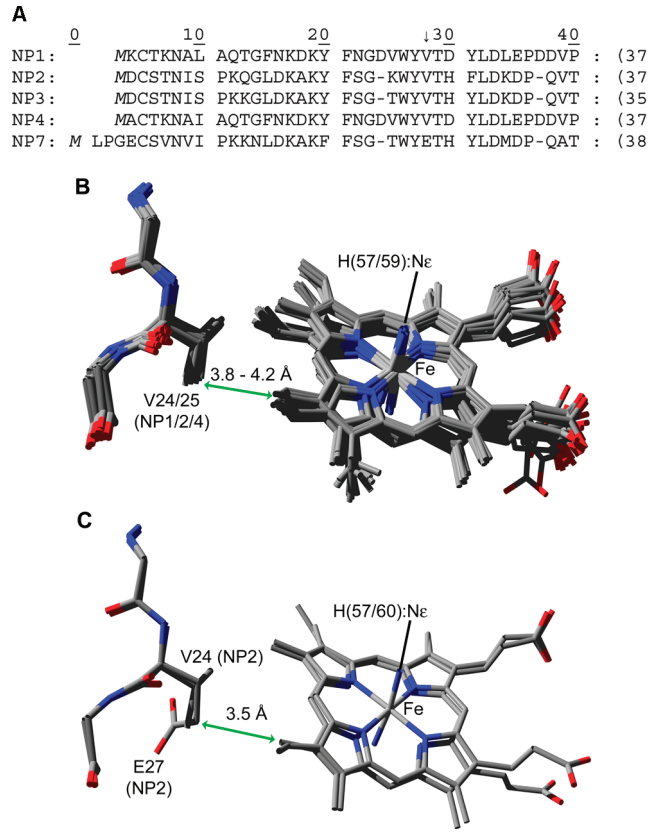

FIGURE 1: (A) Alignment of the N-terminal amino acid sequences of recombinant NP1−4 and NP7 from *R. prolixus*. The positions of residue Glu-27 in NP7 and the corresponding Val in NP1−4 are indicated by the arrow. (B) Relative positions of Val-24/25 with respect to the heme in the 31 X-ray structures of *wt* NP1 (PDB entries 4NP1, 1NP1, 2NP1, and 3NP1), *wt* NP2 (PDB entries 1EUO, 1T68, 2HYS, 1PEE, 2AH7, 2AL0, 2A3F, 2ACP, 1GTF, 2EU7, and 2ASN), and *wt* NP4 (PDB entries 1D3S, 1U0X, 1D2U, 1NP4, 1X8P, 1X8N, 1KOI, 1X8O, 1YWB, 1X8Q, 1YWD, 1IKE, 1IKJ, 1ML7, 1YWA, and 1YWC) currently available from the Protein Data Bank. (C) Comparison between the structure of NP2 with heme in the **B** orientation (PDB entry 1EUO) (*17*) and the homology model of NP7(G3−S182) with a symmetrical heme inserted (*16*). Note that the view of the structures is from the proximal side of the cofactor. Figures were prepared with DEEPVIEW version 3.7 (*39*) (available at http://www.expasy.org/spdbv/) and rendered with POV-RAY version 3.6 (available at http://www.povray.org/).

EXPERIMENTAL PROCEDURES

Mutants of NP7 (pNP7^{Kan} plasmid) and NP2 (pNP2^{Kan} plasmid) (*7, 12*) were generated by the quick change mutagenesis method (*18*) using *Pfu* DNA polymerase (Stratagene). The following pairs of primers were used: for pNP7E27V^{Kan}, 5′-TTC AGC GGT ACT TGG TAT GTT ACT CAT TAT CTA GAC ATG-3′ and 3′-AAG TCG CCA TGC ACC ATA CAA TGA GTA ATA GAT CTG TAC-5′; for pNP7E27Q^{Kan}, 5′-TTC AGC GGT ACT TGG TAT CAG ACT CAT TAT CTA GAC ATG-3′ and 3′-AAG TCG CCA TGA ACC ATA GTC TGA GTA ATA GAT CTG TAC-5′; for pNP2V24E^{Kan}, 5′-TTC AGC GGT AAA TGG TAT GAA ACC CAC TTC CTG GAC AAG-3′ and 3′-AAG TCG CCA TTT ACC ATA CTT TGG GTG AAG GAC CTG TTC-5′ (the sites of mutation are underlined). The correctness of the coding regions of all expression plasmids was confirmed through DNA sequencing.

Prior to expression, plasmids were transformed into *Escherichia coli* strain BL21(DE3) (Novagen). NP2 and

NP2(V24E) were expressed, reconstituted, and purified as described previously for NP2 (*7*) and NP7 (*12*). The other proteins were reconstituted by a stepwise heme insertion described for the preparation of NP7 (*12*). The protein preparations were judged by SDS−PAGE to be ∼90% pure. Proteins were also subjected to MALDI-TOF MS to confirm the correct molecular masses (calculations consider an initial Met-0 and assume the presence of two Cys−Cys disulfides): calcd for $[NP7(E27V) + H]^+$ 20939 Da, observed 20939 ± 10 Da; calcd for $[NP7(E27Q) + H]^+$ 20969 Da, observed 20975 ± 10 Da; calcd for $[NP2(V24E) + H]^+$ 20080 Da, observed 20070 ± 10 Da. Proteins were stored at −20 °C in 200 mM NaO*Ac*/HO*Ac* and 10% (v/v) glycerol (pH 5.0) until use.

For the buffered NMR solutions, exchangeable protons in Na_2HPO_4 and ImH were exchanged against deuterons by three solvation−freeze-dry cycles with D_2O. The pH was then adjusted through titration with acetic acid-d_4 using a standard pH electrode (H_2O); pH values are not corrected for the deuterium isotope effect (designated pH*). Protein samples for NMR in 100 mM NaO*Ac*/HO*Ac* (pH 5.0) were concentrated using Biomax ultrafiltration concentrators (NMWL 10 kDa) (Millipore). Buffer was exchanged through extensive washing (three times) with a 30 mM Na_2DPO_4/acetic acid-d_4 mixture in D_2O (pH* 5.5) in the same ultrafiltration devices. *wt* NP2 samples were prepared from lyophilisates as previously described (*5, 6, 9, 10*). NMR samples finally consisted of 1−2 mM protein solutions. To obtain the low-spin complexes, protein samples were mixed with excess ImD/acetic acid-d_4 mixture in D_2O (pH* 5.5). NMR data were collected over the temperature range of 25−35 °C with the chemical shift referenced to residual water on Bruker DRX-500 and Bruker DRX-600 spectrometers operating at 499.58 and 600.13 MHz proton Larmor frequency, respectively.

Circular dichroism (CD) measurements were performed at 19 ± 1 °C using a Jasco (model J-810) spectropolarimeter in quartz cuvettes with a path length of 1 or 0.2 cm. Samples were dissolved in 20 mM NaO*Ac*/HO*Ac* (pH 5.0) and subsequently diluted (1:20) into 100 mM MOPS/NaOH (pH 7.5), where 2 mM histamine·HCl or sodium (*Z*)-1-(*N*,*N*-diethylamino)diazen-1-ium-1,2-diolate (DEA/NO) was added. Four to six spectra were accumulated for each sample, and values were normalized to the protein concentration upon baseline subtraction. The instrument determines the ellipticity θ, in millidegrees, which was converted into the molar extinction by the equation

$$\Delta\varepsilon = \frac{4\pi\theta}{180 \times \ln(10) \times Cl} = \frac{\theta}{32.982Cl}$$

where *C* is the sample concentration (in moles per liter) and *l* the cuvette path length (in centimeters) (*19*).

RESULTS

The three novel mutants and the NP2 and NP7 *wt* proteins were expressed, refolded, and reconstituted as previously described (*7, 12*). All apoproteins readily took up the heme cofactor and showed absorption spectra similar to those of the other NPs. All proteins were capable of binding NO, Hm, and imidazole (ImH). NP7(E27Q) was significantly labilized; i.e., at high concentrations, the protein precipitated and was, therefore, not investigated by NMR spectroscopy. The integrity of the other proteins was occasionally monitored by ^{1}H NMR spectroscopy and compared with earlier spectra of the same sample. However, as reported previously, the recording of ^{1}H NMR spectra of the *wt* NP7−ImH species requires the adjustment of the pH* to 5.5 to produce reasonably resolved spectra at 25 °C (*16*). Dynamic light scattering experiments revealed that the largest fraction in the NP7 NMR samples was indeed in an oligomeric state (*16*). This effect is ascribed to the strong charge dipolar nature of NP7, i.e., 16 surface carboxylates (of 25 total) on the side of the entrance of the heme pocket and 16 surface Lys residues (of 27 total) at the opposite side. As a consequence, NP7 forms oligomers at the concentrations required for NMR spectroscopy which are thus expected to tumble more slowly in the NMR sample solution and, thus, result in decreased spin−spin relaxation times (T_2) (*16*). To further improve the spectral quality, one-dimensional (1D) ^{1}H NMR spectra were recorded at various temperatures. It was found that the smallest line widths ($\Delta\nu$) were obtained at 35−40 °C, which was then used as the temperature range for further investigations.

1D ^{1}H NMR spectra of NP2, NP2(V24E), NP7(E27V), and NP7 at pH* 5.5 are presented in Figure 2 without and with ImH added. The high-spin species exhibit resonances between 80 and −20 ppm; however, only NP2, NP2(V24E), and NP7(E27V) have resolved hyperfine-shifted ferriheme proton resonances, and the quality of the spectra drops dramatically in this order (Figure 2A). Resonances of NP2 were assigned on the bases of the previous assignments of the very similar spectra at pH* 7.0 (*5, 10*). Few resonances were attributed to **A** in the presence the dominating **B**. By integration of the corresponding methyl resonances, a slight increase in the **A**:**B** ratio was observed at the lower pH* (Table 1). Remarkably, the ^{1}H NMR spectrum of NP2(V24E) at pH* 5.5 shows a completely different resonance pattern compared to that of NP2, with a tendency toward larger chemical shifts for all ferriheme signals. Previous NMR studies on NP1, -2, and -4 containing heme *b* showed that the resonances of the **A** isomer generally appear at larger proton chemical shifts compared to those of the **B** isomer (*8*). Thus, it is reasonable to assume, from the larger chemical shifts of the NP2(V24E) mutant, that this species may have the **A** heme orientation, and this has been confirmed by the spectra of the low-spin complexes. Unfortunately, assignments for NP7 and NP7(E27V) were not possible because of the broad lines. However, interestingly, the spectra show that the replacement of Glu-27 in NP7 reduces the line widths, $\Delta\nu$, whereas the insertion of Glu-24 in NP2 increases $\Delta\nu$.

NMR spectra of the ImH complexes were much better resolved (Figure 2B), and the resonances range from 30 to −10 ppm. As is the case with the spectra of the high-spin compounds, the major chemical shifts of the NP2−ImH species at pH* 5.5 do not differ very much from those obtained at pH* 7.0 (*5*). For a complete assignment of the heme resonances, ^{1}H−^{13}C HMQC and ^{1}H WEFT-NOESY spectra were recorded and are presented in Figures S1 and S2 of the Supporting Information. The **A**:**B** ratio increased slightly with a decrease in pH* (Table 1). Moreover, a series of at least four small resonances of a minor species appeared between 24 and 19 ppm. These are currently under further

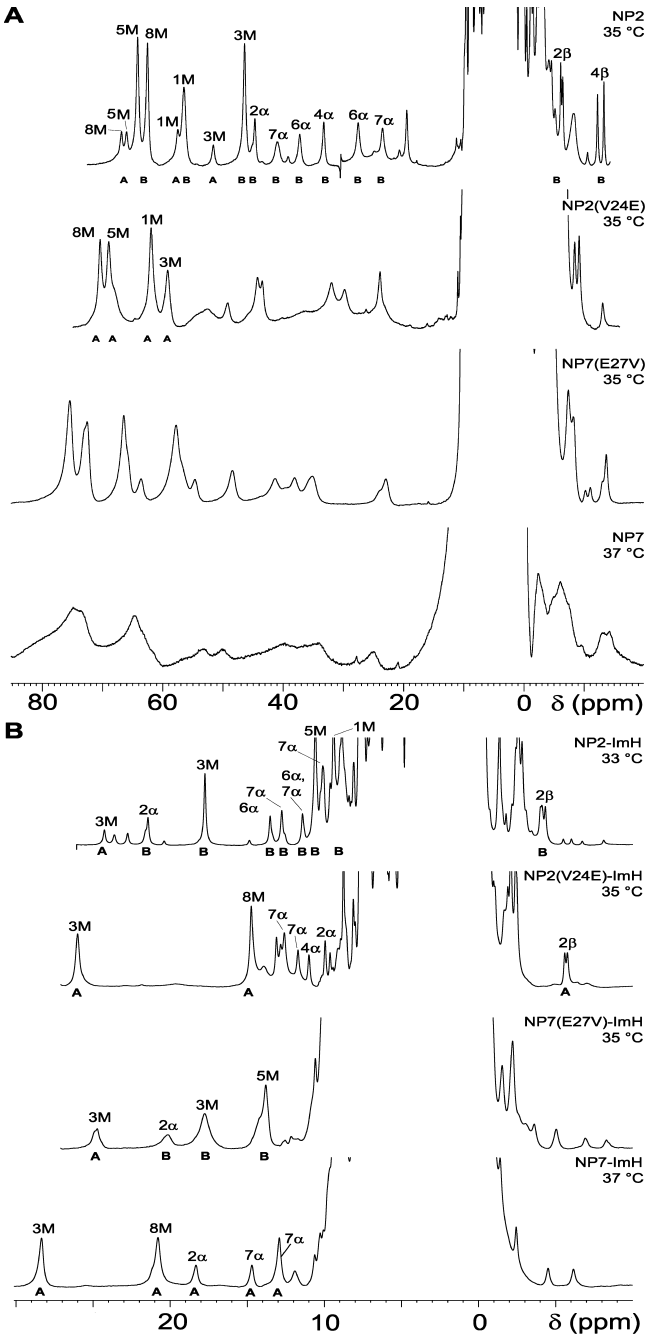

FIGURE 2: ^{1}H NMR spectra of *R. prolixus* NP2, NP2(V24E), NP7(E27V), and NP7 in D_2O, buffered with a 30 mM Na_2DPO_4/acetic acid-d_4 mixture (pH* 5.5). (A) Spectra of the high-spin complexes (no ligand added; $S = {}^5/_2$). (B) Spectra of the low-spin complexes with ImH as the axial ligand ($S = {}^1/_2$) (1M, 3M, 5M, and 8M for heme methyl protons, 2α, 4α, 2β, and 4β for heme vinyl $C^{\alpha}H$ and $C^{\beta}H_2$ groups, and 6α and 7α for the propionate $C^{\alpha}H_2$ groups; numbering corresponds to the pyrrole ring β-carbons according to Scheme 1; **A** and **B** designate the two different heme orientations that have been assigned).

investigation (F. Yang, M. Knipp, and F. A. Walker, work in progress).

Besides slightly increased line widths, $\Delta\nu$, the spectrum of the NP2(V24E)−ImH species exhibits a remarkably changed resonance pattern compared to that of the NP2−ImH species with 2α at much smaller chemical shift than 3M which typically indicates the **A** orientation of the NPs (*20*). As for the high-spin form, the larger chemical shifts are consistent with the predominance of the **A** isomer. Furthermore, the ^{1}H−^{13}C HMQC and ^{1}H WEFT-NOESY spectra of the NP2(V24E)−ImH species were recorded and are displayed in Figures S3 and S4 of the Supporting Information. These spectra allow the complete assignment of the heme proton resonances (Table S2 of the Supporting Information). Thus, the Val → Glu mutation completely reversed the orientation of the heme *b* cofactor from **B** to **A**, with no detectable **B** being present.

Table 1: Comparison of the Ratios of the **A** and **B** Heme Orientations in NP2 and NP7 from *R. prolixus* and Several Mutants at Equilibrium

	A:**B** ratio		
	distal ligand: H_2O[a]	NH_3	ImH
NP2, pH* 7.0[b]	1:8 (*5*)	1:8 (*5*)	1:6 (*7*)
NP2, pH* 5.5[b]	1:5		1:5
NP2(V24E), pH* 5.5[b]	**A**[c]		**A**[c]
NP7(E27V), pH* 5.5[b]			1:3
NP7(E27Q), pH 5.0[d]			**A**[c]
NP7, pH* 5.5[b]			**A**[c]

[a] No ligand added. [b] Determined by NMR spectroscopy (numbers obtained by integration). [c] Only **A** detectable. [d] Determined by CD spectroscopy.

The spectral resolution of the NP7−ImH complex is significantly improved compared to that of its high-spin form, but broad lines were still observed. Previously, we proposed that the NP7−ImH complex contains **A** on the basis of the fact that large chemical shifts was indicative of **A** in NP1−4 (*16, 21*). Only two heme methyl peaks are shifted out of the diamagnetic proton region. Thus, it can be concluded that the 5M and 1M resonances, which always appear together within a relatively small chemical shift difference, are the resonances hidden under the protein proton envelope (*5*−*10*). The shift pattern obtained for the NP7−ImH complex in 1D ^{1}H NMR is similar to that of the NP2(V24E)−ImH complex (Figure 2B); i.e., 3M has the largest chemical shift followed by 2α, which is always the case for NP−ImH complexes with the heme in the **A** orientation (*9*). Furthermore, in the ^{1}H WEFT-NOESY spectrum, the assignments of the 3M and 2α resonances were verified by both showing cross-peaks to the *meso*-α proton; in the same spectrum, the assignment of the 8M resonance was verified by the cross-peak obtained with the 7α protons (Figure S5 of the Supporting Information). In contrast, the ^{1}H resonance pattern of the NP7(E27V)−ImH complex is again similar to that of the NP2−ImH complex, therefore suggesting the presence of the $3M_{\mathbf{A}}$ resonance at the highest chemical shift followed by the $2\alpha_{\mathbf{B}}$ resonance, which typically precedes the $3M_{\mathbf{B}}$ resonance in NPs (*5*−*10*).

Extrinsic chromophores, such as the *b*-type heme molecule, are not optically active, but their interaction with the chiral environment of the protein matrix upon binding generates optical activity (*22*−*25*). The reason for the induction of optical activity to the heme cofactor is ascribed to the coupling oscillator interactions of the heme $\pi \rightarrow \pi^*$ transitions, which are identified as the cause of Soret absorption, with (i) nearby aromatic site chains, (ii) the peptide backbone, and (iii) out-of-plane distortion of the cofactor (*23, 24*). Figure 3 shows the circular dichroism (CD) spectra of the Soret band region of NP2, NP2(V24E), NP7(E27V), NP7(E27Q), and NP7 recorded in the presence of either excess Hm or NO (produced from the NO-releasing compound DEA/NO). Interestingly, in both low-spin forms,

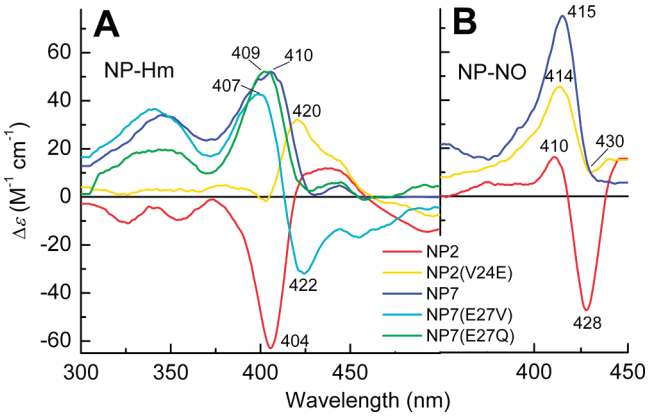

FIGURE 3: Circular dichroism (CD) spectra of the Soret band region of NP7, NP7(E27V), NP7(E27Q), NP2(V24E), and NP2: (A) Hm complexes and (B) NO complexes. Numbers denote the wavelengths, in nanometers, of spectral maxima and minima.

NP2 (mainly **B** orientation) exhibited an almost exclusively negatively polarized $\Delta\varepsilon$, whereas NP2(V24E) (**A** orientation) exhibited a positive polarization. Furthermore, the orientation reversal induced a significant difference in the absorption maximum ($\leq$16 nm). The dependence of the CD polarization and absorption maxima on the heme orientation was previously reported for Mb and hemoglobin (Hb) (*22*−*25*). Both proteins have a strong preference for one heme orientation; therefore, measurements on the less favored orientation have been estimated from measurements under nonequilibrium conditions, which is possible because of the slow equilibration rate in the range of hours to days (*26*).

In the case of NP7, a similar trend in polarization was observed, thus supporting the NMR assignment given above as the **A** orientation, whereas the mixed species observed in NP7(E27V) is probably a result of maxima occurring in both polarizations. The sharp bands obtained for the nitrosyl complexes with minor maxima in the opposite polarization to the major orientation may reflect the occurrence of the mixed orientations for NP2 and NP2(V24E), which was also observed for NP2 by NMR. On the basis of these results, CD also allowed identification of the heme orientation of the NP7(E27Q)−Hm complex because of the much smaller concentrations required as compared to NMR. The CD spectra allowed us to conclude that NP7(E27Q) favors the **A** orientation as does *wt* NP7. This particular mutation, thus, allows two further conclusions. (i) The large difference between Gln and Glu in terms of stability indicates the importance of the charge for the proper protein fold and functions of NP7 and further allows the conclusion that Glu-27 is indeed deprotonated ($pK_a < 5$). (ii) The similar behavior in CD spectroscopy, reflecting the same orientation, provides evidence that it is the steric properties of Glu-27 rather than its charge which leads to the reversed orientation of the cofactor. This is strongly supported by the 0.3 Å smaller distance of Glu-27 $C^{\gamma} \leftrightarrow heme_B$ 2-vinyl-C^{β} (3.2 Å) compared to Glu-27 $C^{\gamma} \leftrightarrow heme_A$ 3-methyl-C in NP7 (3.5 Å) (Figure 1C).

DISCUSSION

Although NP1−4 have been extensively studied and are structurally and functionally well-characterized, it remains a matter of debate why the saliva of the so-called "kissing bug" (*R. prolixus*) contains a cocktail of five to eight nitrophorins (*27*) instead of just one, which apparently is the case with *Cimex lectularius* (the bedbug) (*28*). In addition, it remains unclear why the six life stages of *R. prolixus* (five instar nymphs and the adult phase) use different patterns of expression of nitrophorins (*29*). To address these questions, comparative investigations of all NPs are required. Furthermore, we want to understand the properties of NP7 as a unique system of delivery of NO to cell surfaces, a field of major importance for the understanding not only of NO physiology but also of drug development (*30*). In addition, to the best of our knowledge, this is the first time that a factor that specifically determines the heme orientation in a protein has been identified.

Of all the *R. prolixus* nitrophorins, NP7 is particularly interesting because it binds to negatively charged cell surfaces (*12, 31*). The gene encoding NP7 has recently been established from a cDNA library generated from salivary glands of V^{th} instar nymphs (*31, 32*). But in contrast to NP1−4, the protein has not been isolated from the insects, perhaps because of the very different pI of NP7, which may have caused it to be missed (*12*). However, as with the other nitrophorins, recombinant expression was shown to be possible (*12*). This not only yields sufficiently large quantities for spectroscopic investigations, such as by NMR spectroscopy (*16*), but also provides access to site-specific mutants, a methodology that is key for carrying out this work and many other studies. Furthermore, the thermodynamic equilibrium for the **A**:**B** ratio in the nitrophorins as well as other proteins studied is in the range of hours to days; for instance, for NP2, $t_{1/2} \approx 2$ h at pH* 7.0, which was determined by NMR spectroscopy (*7*). Unfortunately, the insertion of heme into NP7 and its mutants, as well as into NP2(V24E), requires slow titration of dilute solutions with hemin, together with continuous removal of excess heme, followed by concentration of the sample, all of which required multiple days to produce the NMR sample (*12*), which did not allow the spectroscopic observation of the kinetics of this process. However, continuous checking of the NMR samples investigated in this study over weeks revealed no changes in the **A**:**B** ratio (data not shown). Because of the expression of NPs, their loading with NO, and the fact that the time span between two applications by the insects is in the time frame of days (*33*), the in vitro data presented reflect the equilibrium situation and, therefore, reflect the in vivo situation.

Here we report on a major sequence difference between NP7 and NP1−4, which has a strong influence on the cofactor orientation. To the best of our knowledge, a similar explanation of the heme rotational disorder as being caused by a single protein residue has previously not been identified. Different rates depending on the heme orientation were, for instance, determined for the O_2 binding to sperm whale Mb (*34*). However, others claim that the heme orientation in Mb does not affect the O_2 affinity (*22, 35*), but differences in possible physiological relevance have been reported for two other heme proteins. A difference of 27 mV in the redox potential of the two isomers of cytochrome b_5 has been found (*36*), and the Bohr effect of *C. thummi thummi* HbIII has been shown to be different for the two isomers (*37*). Furthermore, heterogeneity in the binding of heme *b* to heme oxygenase from *Pseudomonas aeruginosa* in both conformations leads to the formation of 70% δ-biliverdin and 30% β-biliverdin (*38*). Therefore, the consideration of the heme orientation and the understanding of the factors that determine the favored site at equilibrium are important for fully

understanding and distinguishing between the properties of the two hemoprotein isomers, **A** and **B**.

Apparently, NP7 is the only *R. prolixus* nitrophorin with a nearly exclusive heme **A** orientation. Further, to the best of our knowledge, this is the first time that a single residue could be shown to have a major responsibility for the stabilization of the heme orientation. The NP2/NP2(V24E) protein pair provides a good starting point for further detailed studies of the factors that determine the orientation of a heme *b* cofactor inside a protein pocket together with the functional and spectroscopic consequences which arise from the two orientations.

ACKNOWLEDGMENT

We are grateful to Prof. F. Ann Walker (The University of Arizona) for helpful discussions and reading of the manuscript. Prof. Milan Vašák (University of Zürich, Zürich, Switzerland) is acknowledged for providing use of the CD instrument.

SUPPORTING INFORMATION AVAILABLE

Figures (S1−S5) and Tables (S1 and S2) mentioned in the text. This material is available free of charge via the Internet at http://pubs.acs.org.

REFERENCES

1. La Mar, G. N., Satterlee, J. D., and de Ropp, J. S. (2000) Nuclear magnetic resonance of hemoproteins. In *The Porphyrin Handbook* (Kadish, K. M., Smith, K. M., and Guilard, R., Eds.) Vol. 5, pp 185−298, Academic Press, San Diego.
2. La Mar, G. N., Davis, N. L., Parish, D. W., and Smith, K. M. (1983) Heme orientational disorder in reconstituted and native sperm whale myoglobin. Proton nuclear magnetic resonance characterization by heme methyl deuterium labeling in the met-cyano protein. *J. Mol. Biol. 168*, 887–896.
3. McLachlan, S. J., La Mar, G. N., Burns, P. D., Smith, K. M., and Langry, K. C. (1986) ^{1}H-NMR assignments and the dynamics of interconversion of the isomeric forms of cytochrome b_5 in solution. *Biochim. Biophys. Acta 874*, 274–284.
4. La Mar, G. N., Smith, K. M., Gersonde, K., Sick, H., and Overkamp, M. (1980) Proton nuclear magnetic resonance characterization of heme disorder in monomeric insect hemoglobin. *J. Biol. Chem. 255*, 66–70.
5. Shokhireva, T. Kh., Shokhirev, N. V., and Walker, F. A. (2003) Assignment of heme resonances and determination of the electronic structures of high- and low-spin nitrophorin 2 by ^{1}H and ^{13}C NMR spectroscopy: An explanation of the order of heme methyl resonances in high-spin ferriheme proteins. *Biochemistry 42*, 679–693.
6. Shokhireva, T. Kh., Berry, R. E., Uno, E., Balfour, C. A., Zhang, H., and Walker, F. A. (2003) Electrochemical and NMR spectroscopic studies of distal pocket mutants of nitrophorin 2: Stability, structure, and dynamics of axial ligand complexes. *Proc. Natl. Acad. Sci. U.S.A. 100*, 3778–3783.
7. Berry, R. E., Shokhireva, T. Kh., Filippov, I., Shokhirev, M. N., Zhang, H., and Walker, F. A. (2007) The effect of the N-terminus on heme cavity structure, ligand equilibrium and rate constants and reduction potentials of nitrophorin 2 from *Rhodnius prolixus*. *Biochemistry 46*, 6830–6843.
8. Shokhireva, T. Kh., Smith, K. M., Berry, R. E., Shokhirev, N. V., Balfour, C. A., Zhang, H., and Walker, F. A. (2007) Assignment of the ferriheme resonances of the high-spin forms of nitrophorins 1 and 4 by ^{1}H NMR spectroscopy: Comparison to structural data obtained from X-ray crystallography. *Inorg. Chem. 46*, 170–178.
9. Shokhireva, T. Kh., Weichsel, A., Smith, K. M., Berry, R. E., Shokhirev, N. V., Balfour, C. A., Zhang, H., Montfort, W. R., and Walker, F. A. (2007) Assignment of the ferriheme resonances of the low-spin complexes of nitrophorins 1 and 4 by ^{1}H and ^{13}C NMR spectroscopy: Comparison to structural data obtained from X-ray crystallography. *Inorg. Chem. 46*, 2041–2056.
10. Shokhireva, T. Kh., Berry, R. E., Zhang, H., Shokhirev, M. N., and Walker, F. A. (2008) Assignment of ferriheme resonances for high- and low-spin forms of nitrophorin 3 by ^{1}H and ^{13}C NMR spectroscopy and comparison to nitrophorin 2: Heme pocket structural similarities and differences. *Inorg. Chim. Acta 361*, 925–940.
11. Walker, F. A. (2005) Nitric oxide interaction with insect nitrophorins and thoughts on the electron configuration of the {FeNO}^{6} complex. *J. Inorg. Biochem. 99*, 216–236.
12. Knipp, M., Zhang, H., Berry, R. E., and Walker, F. A. (2007) Overexpression in *Escherichia coli* and functional reconstitution of the liposome binding ferriheme protein nitrophorin 7 from the blood sucking bug *Rhodnius prolixus*. *Protein Expression Purif. 54*, 183–191.
13. Lehane, M. J. (2005) *The Biology of Blood-Sucking in Insects*, 2nd ed., Cambridge University Press, Cambridge, United Kingdom.
14. Montfort, W. R., Weichsel, A., and Andersen, J. F. (2000) Nitrophorins and related antihemostatic lipocalins from *Rhodnius prolixus* and other blood-sucking arthropods. *Biochim. Biophys. Acta 1482*, 110–118.
15. Weichsel, A., Andersen, J. F., Roberts, S. A., and Montfort, W. R. (2000) Nitric oxide binding to nitrophorin 4 induces complete distal pocket burial. *Nat. Struct. Biol. 7*, 551–554.
16. Knipp, M., Yang, F., Berry, R. E., Zhang, H., Shokhirev, M. N., and Walker, F. A. (2007) Spectroscopic and functional characterization of nitrophorin 7 from the blood-feeding insect *Rhodnius prolixus* reveals an important role of its isoform-specific N-terminus for proper protein function. *Biochemistry 46*, 13254–13268.
17. Andersen, J. F., and Montfort, W. R. (2000) The crystal structure of nitrophorin 2. A trifunctional antihemostatic protein from the saliva of *Rhodnius prolixus*. *J. Biol. Chem. 275*, 30496–30503.
18. Wang, W., and Malcolm, B. A. (1999) Two-stage PCR protocol allowing introduction of multiple mutations, deletions and insertions using QuikChange Site-Directed Mutagenesis. *BioTechniques 26*, 680–682.
19. Rodger, A., and Nordén, B. (1997) *Circular Dichroism and Linear Dichroism*, Vol. 1, 1st ed., Oxford University Press, Oxford, United Kingdom.
20. Shokhirev, N. V., and Walker, F. A. (1998) The effect of axial ligand plane orientation on the contact and pseudocontact shifts of low-spin ferriheme proteins. *J. Biol. Inorg. Chem. 3*, 581–594.
21. Shokhirev, N. V., and Walker, F. A. (1998) Co- and counterrotation of magnetic axes and axial ligands in low-spin ferriheme systems. *J. Am. Chem. Soc. 120*, 981–990.
22. Aojula, H. S., Wilson, M. T., and Drake, A. (1986) Characterization of haem disorder by circular dichroism. *Biochem. J. 237*, 613–616.
23. Kiefl, C., Sreerama, N., Haddad, R., Sun, L., Jentzen, W., Lu, Y., Qui, Y., Shelnutt, J. A., and Woody, R. W. (2002) Heme distortion in sperm-whale carbonmonoxy myoglobin: Correlations between rotational strengths and heme distortions in MD-generated structures. *J. Am. Chem. Soc. 124*, 3385–3394.
24. Woody, R. W., Kiefl, C., Sreerama, N., Lu, Y., Qui, Y., and Shelnutt, J. A. (2002) MD simulations of carbonmonoxy myoglobin and calculations of heme CD. In *Insulin & Related Proteins: Structure to Function and Pharmacology* (Federwisch, M., Dieken, M. L., and De Meyts, P., Eds.) pp 233−248, Kluwer Academic Publishers, Dordrecht, The Netherlands.
25. Nagai, M., Nagai, Y., Aki, Y., Imai, K., Wada, Y., Nagatomo, S., and Yamamoto, Y. (2008) Effect of reversed heme orientation on circular dichroism and cooperative oxygen binding of human adult hemoglobin. *Biochemistry 47*, 517–525.
26. Santucci, R., Ascoli, F., La Mar, G. N., Parish, D. W., and Smith, K. M. (1990) Horse heart myoglobin reconstituted with a symmetrical heme: A circular dichroism study. *Biophys. Chem. 37*, 251–255.
27. Soares, R. P. P., Sant'Anna, M. R. V., Gontijo, N. F., Romanha, A. J., Diotaiuti, L., and Pereira, M. H. (2000) Identification of morphologically similar *Rhodnius* species (Hemiptera: Reduviidae: Triatominae) by electrophoresis of salivary heme proteins. *Am. J. Trop. Med. Hyg. 62*, 157–161.
28. Weichsel, A., Maes, E. M., Andersen, J. F., Valenzuela, J. G., Shokhireva, T. K., Walker, F. A., and Montfort, W. R. (2005) Heme-assisted S-nitrosation of a proximal thiolate in a nitric oxide transport protein. *Proc. Natl. Acad. Sci. U.S.A. 102*, 594–599.
29. Moreira, M. F., Coelho, H. S. L., Zingali, R. B., Oliveira, P. L., and Masuda, H. (2003) Changes in salivary nitrophorin profile during the life cycle of the blood-sucking bug *Rhodnius prolixus*. *Insect Biochem. Mol. Biol. 33*, 23–28.
30. Knipp, M. (2006) How to control NO production in cells: N^{ω},N^{ω}-dimethyl-L-arginine dimethylaminohydrolase as a novel drug target. *ChemBioChem 7*, 879–889.

31. Andersen, J. F., Gudderra, N. P., Francischetti, I. M. B., Valenzuela, J. G., and Ribeiro, J. M. C. (2004) Recognition of anionic phospholipid membranes by an antihemostatic protein from a blood-feeding insect. *Biochemistry 43*, 6987–6994.

32. Ribeiro, J. M. C., Andersen, J. F., Silva-Neto, M. A. C., Pham, V. M., Garfield, M. K., and Valenzuela, J. G. (2004) Exploring the sialome of the blood-sucking bug *Rhodnius prolixus*. *Insect Biochem. Mol. Biol. 34*, 61–79.

33. Nussenzveig, R. H., Bentley, D. L., and Ribeiro, J. M. C. (1995) Nitric oxide loading of the salivary nitric-oxide-carrying hemoproteins (nitrophorins) in the blood-sucking bug *Rhodnius prolixus*. *J. Exp. Biol. 198*, 1093–1098.

34. Livingston, D. J., Davis, N. L., La Mar, G. N., and Brown, W. D. (1984) Influence of heme orientation on oxygen affinity in native sperm whale myoglobin. *J. Am. Chem. Soc. 106*, 3026–3027.

35. Light, W. R., Rohls, R. J., Palmer, G., and Olson, J. S. (1987) Functional effects of heme orientational disorder in sperm whale myoglobin. *J. Biol. Chem. 262*, 46–52.

36. Walker, F. A., Emrick, D., Rivera, J. E., Hanquet, B. J., and Buttlaire, D. H. (1988) Effect of heme orientation on the reduction potential of cytochrome b_5. *J. Am. Chem. Soc. 110*, 6234–6240.

37. La Mar, G. N., Overkamp, M., Sick, H., and Gersonde, K. (1978) Proton nuclear magnetic resonance hyperfine shifts as indicators of tertiary structural changes accompanying the Bohr effect on monomeric insect hemoglobins. *Biochemistry 17*, 352–361.

38. Rivera, M., and Zeng, Y. (2005) Heme oxygenase, steering dioxygen activation toward heme hydroxylation. *J. Inorg. Biochem. 99*, 337–354.

39. Guex, N., and Peitsch, M. C. (1997) SWISS-MODEL and the Swiss-PdbViewer: An environment for comparative protein modeling. *Electrophoresis 18*, 2714–2723.

BI8020229